Medical Engineering & Physics 36 (2014) 102–109

Contents lists available at ScienceDirect

Medical Engineering & Physics

journal homepage: www.elsevier.com/locate/medengphy

Multidirectional quantification of trunk stiffness and damping during unloaded natural sitting

Albert H. Vette[a,b], Kei Masani[c,d,*], Noel Wu[c,d], Milos R. Popovic[c,d]

[a] Department of Mechanical Engineering, University of Alberta, 4-9 Mechanical Engineering Building, Edmonton, Alberta T6G 2G8, Canada
[b] Glenrose Rehabilitation Hospital, 10230 111 Avenue NW, Edmonton, Alberta T5G 0B7, Canada
[c] Institute of Biomaterials and Biomedical Engineering, University of Toronto, 164 College Street, Toronto, Ontario M5S 3G9, Canada
[d] Lyndhurst Centre, Toronto Rehabilitation Institute, 520 Sutherland Drive, Toronto, Ontario M4G 3V9, Canada

ARTICLE INFO

Article history:
Received 3 January 2013
Received in revised form
20 September 2013
Accepted 10 October 2013

Keywords:
Balance
Damping
Human
Mathematical model
Motor control
Optimization
Sitting
Stiffness
System identification
Trunk

ABSTRACT

Trunk instability during sitting is a major problem following neuromuscular injuries such as stroke and spinal cord injury. In order to develop new strategies for alleviating this problem, a better understanding of the intrinsic contributions of the healthy trunk to sitting control is needed. As such, this study set out to propose and validate a novel methodology for determining multidirectional trunk stiffness during sitting using randomized transient perturbations. Fifteen healthy individuals sitting naturally on a custom-made seat were randomly perturbed in eight horizontal directions. Trunk stiffness and damping were quantified using force and trunk kinematics in combination with translational and torsional models of a mass-spring-damper system. The results indicate that stiffness and damping of the healthy trunk are roughly symmetrical between the two body sides. Moreover, both quantities are smallest in the anterior and largest in the lateral directions. In conclusion, a novel protocol for identifying intrinsic trunk stiffness and damping has been developed, eliminating anticipation effects with respect to perturbation timing and direction. Subsequent studies will use these findings as a reference not only for quantifying trunk stiffness and damping in individuals with various neuromuscular disorders, but also for assessing whether neuroprostheses could increase upper body stiffness and, hence, stability.

1. Introduction

Trunk instability is a major problem for people with neuromuscular disorders affecting the transmission and integration of sensorimotor information. It not only compromises their independence during activities of daily living (ADL) [1,2], but can also lead to secondary health complications such as kyphosis, pressure sores, and reduced respiratory capacity [3–5]. Consequently, it is not surprising that, for example, people with spinal cord injury (SCI) prioritize the recovery of trunk stability over the recovery of walking function [6]. Furthermore, trunk stability has recently been identified as the key factor in human balance control and mobility, regardless of the movement or task to be completed. This can be ascribed to the fact that over half of the body's mass is located above the pelvis [7]. As a consequence, the ability to balance the trunk is critical for maintaining stability of the entire body [8] during sitting, standing, walking, and other ADL.

While the topic of trunk stability has enjoyed much attention in the scientific literature, the primary focus has been on inter-vertebral stability (e.g., in the context of low back pain or injury) [9–11], rather than on postural stability. Considering that the human spine is inherently unstable, however, the trunk musculature is pivotal for maintaining the upper body's postural integrity against various environmental challenges related to (1) increased loading (e.g., during object lifting) and (2) transient perturbations (e.g., during a subway/train ride). In particular, the trunk's stability against increased loading is ensured by co-activating the musculature surrounding the spine, resulting in increased multidirectional stiffness [12]. Such an increase in muscle stiffness has additionally been demonstrated to contribute to trunk stabilization against transient lateral perturbations [13–15].

Generally, the muscle stiffness required to complement direction-specific joint (or inter-vertebral) stiffness to overcome postural challenges consists of two components: intrinsic and reflex stiffness. On the one hand, *intrinsic stiffness* is determined by the mechanical properties of the muscle-tendon complex and the pre-activated trunk musculature (open-loop control) [16]. On the other hand, *reflex stiffness* is generated in response to a perturbation via neural reflex pathways (closed-loop control) and is proportional to the angular change at the joint [17–19]. For large

* Corresponding author at: Rehabilitation Engineering Laboratory, Lyndhurst Centre, Toronto Rehabilitation Institute, 520 Sutherland Drive, Toronto, Ontario M4G 3V9, Canada. Tel.: +1 416 597 3422x6098; fax: +1 416 425 9923.
E-mail address: k.masani@utoronto.ca (K. Masani).

1350-4533/$ – see front matter © 2013 IPEM. Published by Elsevier Ltd. All rights reserved.
http://dx.doi.org/10.1016/j.medengphy.2013.10.005

perturbations, the contribution of reflex stiffness is essential for the maintenance of trunk stability [20]. For gentle perturbations, however, tonic pre-activation of the trunk musculature (i.e., intrinsic stiffness) may already suffice for trunk stability, alleviating the need for further reflex-driven and direction-specific activation of the musculature [14,21].

In the context of trunk stability, the intrinsic stiffness of the spine and trunk musculature can be assessed globally by quantifying the stiffness of the trunk itself. When perturbed by a small force, the trunk has been shown to behave like a mass-spring-damper system [22]. Using this representation, the stiffness of the trunk can be 'reverse-engineered' by measuring externally applied forces and the resulting trunk kinematics (*system identification*). Various studies have estimated trunk stiffness for one or more perturbation directions, and this under loaded and/or unloaded conditions [13,15,22,23]. No study, however, has utilized the *same* experimental procedures and conditions to identify *translational* and *torsional* estimates of trunk stiffness during the natural (unloaded) *sitting* posture for *all* anterior–posterior, lateral, and diagonal directions (total of eight directions). Since trunk stiffness is believed to vary depending on the direction of trunk deflection, such a study may be important for better understanding the contribution of intrinsic trunk stiffness to sitting stability during ADL and for developing neuroprostheses for people with neuromuscular disorders. Based on these considerations, the purpose of this study was to: (1) propose and validate a novel methodology for accurately and efficiently determining multidirectional trunk stiffness during sitting (translational and torsional estimates); and (2) identify a control set of such stiffness values for healthy and young individuals as a benchmark for future studies with different populations, e.g., individuals with SCI or stroke.

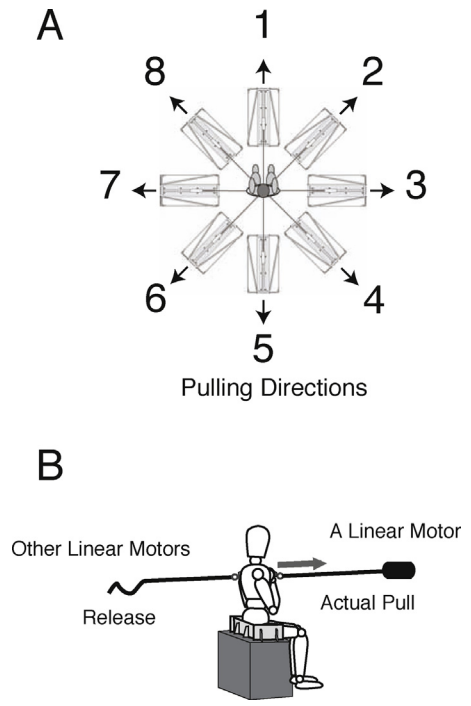

Fig. 1. Schematic of the eight different perturbation directions (A) and the applied perturbation concept (B). The PAPPS delivered horizontal perturbations in the following directions: anterior (1), anterior-right (2), right (3), posterior-right (4), posterior (5), posterior-left (6), left (7), and anterior-left (8). During each trial, a randomly determined PAPPS unit displaced the subject's trunk by 2 cm, while the remaining seven units moved toward the subject to prevent any form of interference with or resistance to the evoked response.

2. Methods

2.1. Subjects

Fifteen healthy and young male individuals were invited to participate in this study (age 26.7 ± 4.6 years; height 176 ± 7 cm; weight 72.5 ± 8.1 kg; mean ± standard deviation). All subjects were free from any prior neurological, vestibular, and sensory impairment as well as from any injuries or disorders of the musculoskeletal system. In addition, none of the subjects reported any prior diagnosis of spinal scoliosis or other conditions affecting seated posture. Each subject gave written informed consent to the experimental procedure, which was approved by the local ethics committee in accordance with the declaration of Helsinki on the use of human subjects in experiments.

2.2. Experimental setup and protocol

Each subject's trunk stiffness and damping were identified using a mathematical description of a second-order mass-spring-damper system in combination with force and kinematics data from perturbation experiments. During the testing, the subject sat on a custom-made sitting apparatus without touching the ground with his feet, had the forearms resting on his lap, and maintained an upright posture with eyes closed. One of the subject's hands held an emergency safety button that, when pressed, shut down the power of the device applying the external perturbation forces to the subject.

To generate the postural perturbations, a custom-made perturbation system, known as the *Portable and Automated Postural Perturbation System* (PAPPS) [24], was used. The PAPPS, which consisted of eight identical perturbation units forming an octagonal structure, delivered horizontal perturbations in the following directions (Fig. 1A): anterior (1), anterior-right (2), right (3), posterior-right (4), posterior (5), posterior-left (6), left (7), and anterior-left (8). The core of each perturbation unit consisted of a linear servo motor (TBX2508-D, Rotalec Inc., Quebec, Canada) that was in series with a load cell (SML 300, Interface Inc., AZ, USA) measuring the pulling force. The linear servo motor controlled the position of the load cell, which was connected to the subject via a short stainless steel cable and a belt harness (Fig. 1B). The harness was secured to the subject's trunk over the trunk segment associated with the tenth thoracic vertebra (T10), which has been suggested to represent the behavior of the center of mass (COM) of the trunk [15]. A motion analysis system (Optotrak 3020, NDI Inc., Ontario, Canada) was used to measure body movement during the perturbations. In order to avoid interference with the perturbation harness, two markers were used to capture the location of the T10 vertebra: one was attached 6 cm below and the other one 6 cm above T10 (*see online supplementary data for justification*). Note that the T10 landmark was identified via palpation by two experienced researchers. All recorded signals were collected with a sampling frequency of 500 Hz and low-pass filtered using a fifth order, zero-phase lag Butterworth filter with a cutoff frequency of 10 Hz [7,21].

The entire perturbation protocol lasted about 15–20 min, with 80 randomized pulls in total and 10 pulls in each direction.[1] Halfway through the experimental session, the subject had a two-minute resting period and was asked to relax his trunk. Prior to each pull, all eight cables applied a projected force of 40 N to the subject.

[1] Note that these 80 'natural' trials alternated with 80 'supported' trials during which constant, low-level functional electrical stimulation (FES) was applied to the abdominal and lower erector spinae muscles. Respective FES-supported results are not subject of the present report.

Note that, as all perturbation cables were taut, each pulling force was canceled out so that the subject was not pulled in a particular direction. Once this quasi-static condition was maintained for a few seconds, an impulsive pulling force was applied in a random horizontal direction. The applied force was induced by a displacement of that direction's servo motor, which had a Gaussian profile with an amplitude of 2 cm and a full width at half maximum of 0.35 s. Note that the optimal perturbation amplitude and duration for evoking small yet distinct trunk displacements were identified in preliminary experiments.[2] While one PAPPS unit was displacing the subject's trunk, the remaining seven units moved toward the subject to prevent any form of interference with or resistance to the evoked response (Fig. 1B). Overall, the subject felt a gentle, but sudden pull in a random direction mimicking an impulse force function. Once each PAPPS unit had returned to its initial position, the next perturbation trial was executed following a random time interval of 1–4 s to prevent anticipation by the subject (which has been shown to significantly influence the neuromuscular state of the trunk and its perturbation response [25]).

2.3. Identification of trunk stiffness and damping

For each executed trial, the kinematics and force data from the first one-second time period following the onset of the perturbation were used in the subsequent system identification. A translational second order system [15] (*Model I*) and a torsional second order system [26] (*Model II*) were used to identify trunk stiffness and damping for each of the eight displacement directions. For *Model I*, the trunk was modeled as a point mass concentrated at the trunk COM, which moved in the horizontal plane and was stabilized by translational stiffness k and damping b. The equation of motion of this system is given by:

$$F = m\ddot{x} + b\dot{x} + kx, \tag{1}$$

where F is the applied force, m is the mass of the trunk, and x, $\dot{x}$, $\ddot{x}$ the linear displacement, velocity, and acceleration of the COM, respectively. The effect of any vertical movement caused by the rotational aspect of the trunk was neglected. For *Model II*, the trunk was again modeled as a point mass concentrated at the trunk COM, which rotated around the spinal joint between the fourth and fifth lumbar vertebrae (L4/L5 joint) [7] and was stabilized by rotational stiffness K and damping B. The equation of motion of this system is given by:

$$\mathrm{FL}\cos\theta + mgL\sin\theta = I\ddot{\theta} + B\dot{\theta} + K\theta, \tag{2}$$

where F denotes the applied force, L the distance between the center of rotation (L4/L5 joint) and the COM of the trunk, m the mass of the trunk, g the acceleration due to gravity, I the moment of inertia of the trunk, and θ, $\dot{\theta}$, and $\ddot{\theta}$ the angular displacement, velocity, and acceleration of the COM, respectively.

The COM was assumed to be located at the T10 vertebral segment [15], the mass of the trunk (m in Eqs. (1) and (2)) was set to 0.563 of the subject's overall mass [7], and I was set to $I = m \times L^2$ [7]. The conversion from the kinematics data series to angular displacement was performed by placing the origin of the coordinate system on the L4/L5 joint and calculating the angle between the time series displacement vector and a constant vertical vector that spans from the L4/L5 joint to the COM in the equilibrium position.

Using the measured force as the input, the stiffness and damping constants (b, k in Eq. (1); B, K in Eq. (2)) were tuned until a good match between the measured and modeled displacement of the trunk COM was achieved. The Gauss-Newton optimization algorithm (Optimization toolbox, Matlab ver. 7.5, Mathworks, MA, USA) governed the search dynamics, whereas the Percentage-of-Fit (%FIT) was used as the cost function for the optimization procedure:

$$\%\mathrm{FIT} = 100\left(1 - \frac{1}{N}\sum_{i=1}^{N}\left|\frac{y_i - Y_i}{y_i}\right|\right), \tag{3}$$

where N is the number of samples, y_i the experimentally measured and Y_i the modeled displacement of the trunk COM [27]. Only stiffness and damping values from models exhibiting a fitting match of 70% or higher were included in the calculation of the mean trunk stiffness and damping for each individual and displacement direction. Note that the perturbation protocol and system identification procedure were validated in a preliminary experiment using a physical mass-spring-damper system with a mass of 3.75 kg, a spring constant of $k = 2.84$ N/mm, and a damping constant of $b = 262.8$ Ns/m (as per manufacturer's specifications) [28].

Using the identified stiffness and damping values, we finally calculated the trunk's undamped natural frequency and damping ratio. The undamped natural frequency ω_0, which is given by:

$$\omega_0 = \sqrt{\frac{k}{m}} \ \text{(translational)} \quad \text{or} \quad \omega_0 = \sqrt{\frac{K}{m}} \ \text{(torsional)}, \tag{4}$$

signifies the frequency at which the undamped system will oscillate when set into motion. The damping ratio ζ, which is given by:

$$\zeta = \sqrt{\frac{b\sqrt{m}}{2m\sqrt{k}}} \ \text{(translational)} \quad \text{or} \quad \zeta = \sqrt{\frac{B\sqrt{m}}{2m\sqrt{K}}} \ \text{(torsional)}, \tag{5}$$

describes how the system returns to its equilibrium after an impulse force is applied. For a damping ratio greater than 1 (*overdamped*), the system will take a longer time to return to equilibrium position than when the damping ratio is equal to 1 (*critically damped*). For a damping ratio between 0 and 1 (*underdamped*), the system will return faster to equilibrium than the overdamped system, but will exhibit small oscillations around the equilibrium point before settling.

2.4. Statistical analysis

For each of the eight displacement directions, the group-average trunk stiffness and damping were identified using the mean values from all subjects. To capture potential differences in group-average stiffness and damping for different displacement directions, a one-way analysis of variance (ANOVA) with repeated measures and a significance level of $\alpha = 0.05$ was performed. Note that the validity of applying the ANOVA to the stiffness and damping values was verified with respect to the underlying assumptions. Following the ANOVA, a Bonferroni post hoc test was used to determine those pairs of displacement direction for which the stiffness and damping values were statistically different from each other ($\alpha = 0.05$). The same analysis was also performed for the trunk's undamped natural frequency, ω_0, and damping ratio, ζ.

3. Results

3.1. Example time series and optimization results

In Fig. 2, representative examples of the perturbation force (A) and the resulting translational (B) and rotational (C) displacement of the trunk COM (gray solid lines) are shown for a single subject and an anterior-left (8) perturbation. Fig. 2B and C also show the modeled displacement of the trunk COM for the translational and

[2] These tests were also used to visually verify that no relative motion between the motion capture markers and the surrounding trunk area occurred.

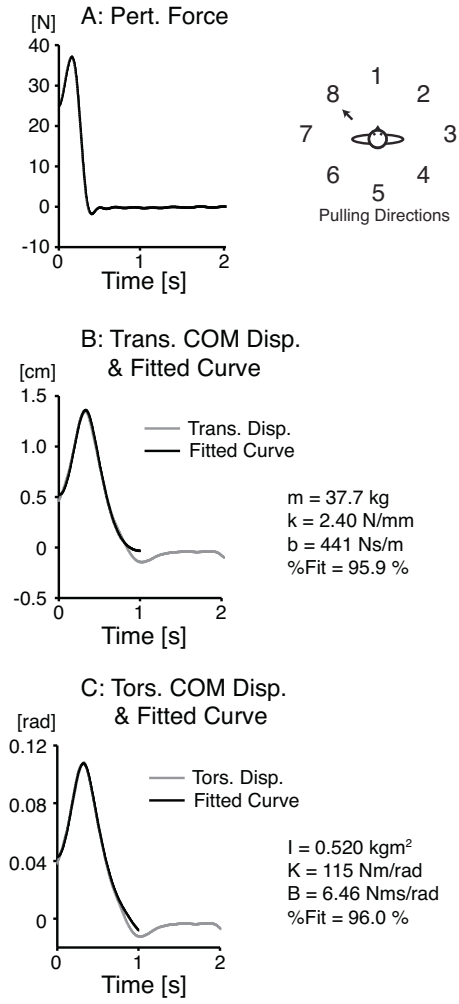

Fig. 2. Representative examples of the perturbation force (A) and the resulting displacement of the trunk COM ((B) translation, (C) rotation; gray solid lines) for a single subject and an anterior-left (8) perturbation. (B and C) Also show the modeled displacement of the trunk COM for the translational and torsional models, respectively (black solid lines). A visual inspection suggests that the modeled COM displacement agreed with the measured COM displacement very well.

torsional models, respectively (black solid lines). A visual inspection suggests that the modeled COM displacement agreed with the measured COM displacement very well, with the translational and torsional models (*Model I*, *Model II*) providing similar, but not identical fits (%FIT = 96%).

Across all subjects, the mean preloading force for all PAPPS units and trials was 37.6 ± 2.7 N (mean ± standard deviation), whereas the peak force at the perturbing PAPPS unit was 39.9 ± 2.4 N for all perturbation directions and trials. From the 1200 trials that were executed in total (15 subjects; 80 trials per subject), less than 0.5% resulted in a Percentage-of-Fit that was lower than 70% (for both Model I and II). The individual stiffness values from the remaining trials, which accounted for a mean Percentage-of-Fit of %FIT = 87.3 ± 6.8% across all subjects, were used to determine the mean trunk stiffness and damping of each individual as a function of trunk displacement direction.

3.2. Translational model results (Model I)

In Fig. 3, the group-average stiffness and damping results are depicted for the translational model (*Model I*). Fig. 3A shows the identified stiffness values and Fig. 3B respective damping values, both as a function of trunk displacement direction. In Fig. 3C and D, the associated undamped natural frequency ω_0 and damping ratio ζ are depicted, respectively.

The applied one-way ANOVA revealed that the stiffness values (Fig. 3A) were significantly different between the eight trunk displacement directions ($p < 0.0001$). The subsequent post hoc analysis indicated that the trunk was significantly stiffer in the lateral directions than in the anterior and posterior directions ($p < 0.05$; horizontal bars in Fig. 3A). In addition, the left (right) direction was found to be significantly stiffer than the anterior-left (anterior-right) direction. When applied to the damping results (Fig. 3B), the ANOVA revealed that also the damping values were significantly different between the eight trunk displacement directions ($p < 0.0001$). The post hoc analysis indicated that the damping was significantly smaller in the posterior direction than in all the other directions, except for the anterior direction (Fig. 3B). In addition, the trunk was significantly more viscous in the lateral directions than in the anterior and posterior directions.

The ANOVA of the undamped natural frequency ω_0 and the damping ratio ζ revealed significant differences across the trunk displacement directions (Fig. 3C and D; $p < 0.0001$). While the bar graph profile for ω_0 generally agreed with the one for trunk stiffness (Fig. 3A and C), ζ showed a more dissimilar profile in comparison with the other plots (Fig. 3D). Note that these observations mirror the different dependencies of ω_0 and ζ on trunk stiffness and damping as described in Eqs. (4) and (5).

3.3. Torsional model results (Model II)

In Fig. 4, the group-average stiffness and damping results are depicted for the torsional model (*Model II*). Fig. 4A shows the identified stiffness values and Fig. 4B respective damping values, both as a function of trunk displacement direction. In Fig. 4C and D, the associated undamped natural frequency ω_0 and damping ratio ζ are depicted, respectively.

The applied one-way ANOVA revealed that the stiffness values (Fig. 4A) were significantly different between the eight trunk displacement directions ($p < 0.0001$). The subsequent post hoc analysis indicated that the trunk was significantly stiffer in the lateral directions than in the anterior and posterior directions ($p < 0.05$; horizontal bars in Fig. 4A). In addition, the left (right) direction was found to be significantly stiffer than the anterior-left (anterior-right) direction. When applied to the damping results (Fig. 4B), the ANOVA revealed that also the damping values were significantly different between the eight trunk displacement directions ($p < 0.0001$). The post hoc analysis indicated that the damping was significantly smaller in the posterior direction than in the lateral and the anterior-left and -right directions (Fig. 4B).

The ANOVA of the undamped natural frequency ω_0 and the damping ratio ζ revealed significant differences across the trunk displacement directions (Fig. 4C and D; $p < 0.0001$). While the bar graph profile for ω_0 generally agreed with the trunk stiffness profile (Fig. 4A and C), ζ showed a more dissimilar profile in comparison with the other plots (Fig. 4D). Note that these observations again mirror the different dependencies of ω_0 and ζ on trunk stiffness and damping as described in Eqs. (4) and (5).

4. Discussion

The present study set out to develop a novel methodology for quantifying multidirectional trunk stiffness and damping during sitting and to identify a control set of such values for healthy and young individuals. In what follows, we elaborate on the validity and characteristics of the developed methodology and discuss the mechanisms and implications of the identified stiffness values only

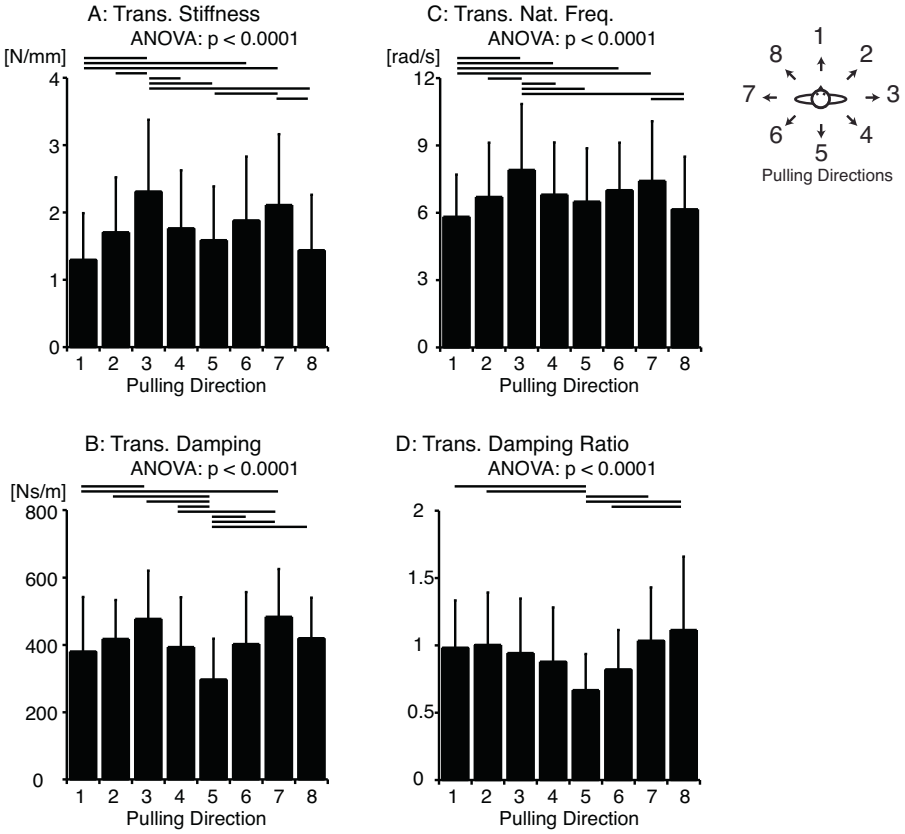

Fig. 3. Stiffness and damping results for the translational model (*Model I*). Shown are the group means ± one standard deviation, for all perturbation directions. (A) Shows the identified stiffness values and (B) respective damping values, both in dependence of trunk displacement direction. In (C and D), the associated undamped natural frequency ω_0 and damping ratio ζ are depicted, respectively. Results of the post hoc multiple comparison are shown using horizontal bars, with the ends of each bar denoting significantly different groups.

(due to their dominant role in trunk stabilization [15,23]) in the context of previous studies on trunk kinetics.

4.1. Validity and characteristics of developed methodology

The adopted perturbation protocol and system identification procedure were validated using a physical mass-spring-damper system [28]. The translational spring and damping constants identified via the optimization technique differed from the actual values by +1.4 ± 3.0% and +1.4 ± 4.4%, respectively (five validation trials). These small discrepancies between the actual and estimated values indicate that the applied perturbation protocol and system identification procedure were, in fact, appropriate for estimating trunk stiffness during sitting. Potential sources for the observed differences may be found in the resolution of the load cell and/or motion capture system, the elasticity in other components of the setup, or the difficulty to manufacture a translational spring with a constant stiffness.

One of the main characteristics of the implemented methodology was that each subject was perturbed in eight different horizontal directions without modifying the experimental arrangement. This was fundamental for providing a control set of multidirectional trunk stiffness values, e.g., for the purpose of developing neuroprostheses for people with SCI. In this context, it should be emphasized that no study to date has identified trunk stiffness and damping in all anterior–posterior, lateral, and diagonal directions. Another characteristic of the experimental protocol was that it utilized randomized perturbation directions and delivery times, thereby eliminating a potential anticipation effect that has been shown to increase co-activation of the trunk musculature prior to perturbations [25]. Finally, considering that the small perturbation amplitude displaced each subject by no more than 2 cm (at the point of application), intrinsic trunk stiffness and damping values could be estimated without eliciting potentially confounding muscle reflexes.

4.2. Direction dependency of human trunk stiffness and damping during sitting

For both the translational and torsional models, trunk stiffness and damping were found to be dependent on perturbation direction. The group-average values reported in Figs. 3 and 4 indicate that both stiffness and damping were smallest in the anterior–posterior displacement directions and largest in the lateral directions. The values for the diagonal directions lay in between these extremes, suggesting that trunk stiffness and damping continuously increase from the anterior (or posterior) to the lateral directions.

The result that trunk *stiffness* during sitting depends on displacement direction can be explained by (1) the anatomy of the spine and (2) the structure of the larger trunk muscles. First, the vertebrae of the spinal column have previously been modeled as deformable segments that are connected by revolute pin joints, facilitating *inter-segmental* spine motion in the anterior–posterior direction only [29]. As lateral spine motion in this model is solely the result of *intra-segmental* deformation, however, the spinal beam is more compliant in the anterior–posterior direction – which is in agreement with the findings presented in Figs. 3A and 4A. In terms of muscle structure, the insertion points of the muscles, the

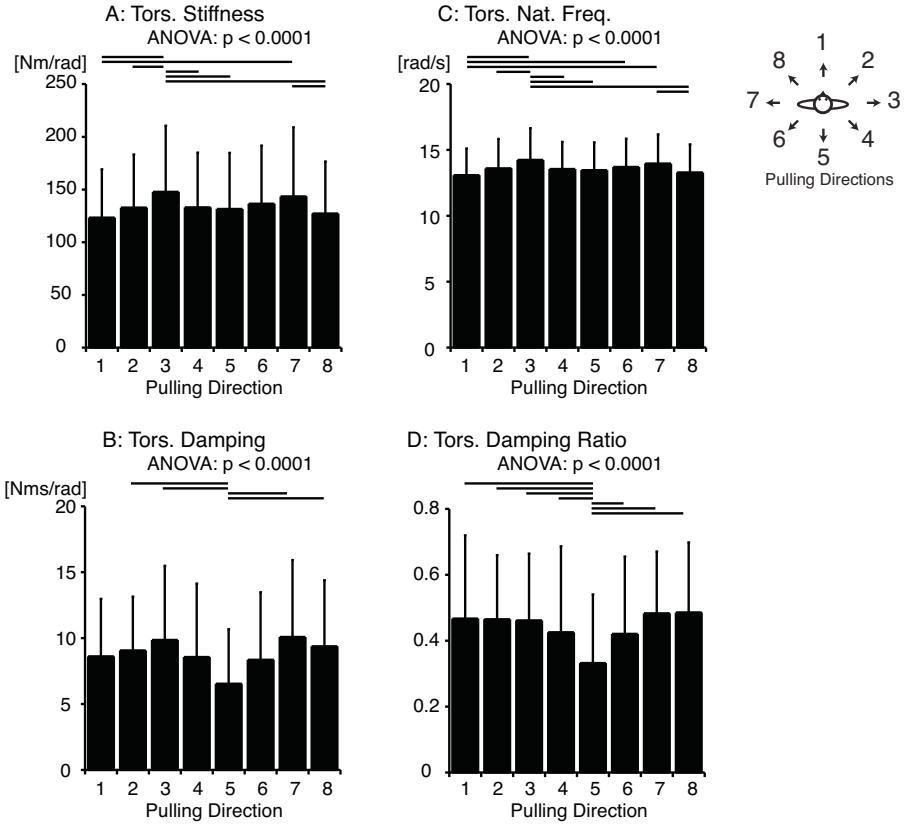

Fig. 4. Stiffness and damping results for the torsional model (*Model II*). Shown are the group means ± one standard deviation, for all perturbation directions. (A) Shows the identified stiffness values and (B) respective damping values, both in dependence of trunk displacement direction. In (C) and (D), the associated undamped natural frequency ω_0 and damping ratio ζ are depicted, respectively. Results of the post hoc multiple comparison are shown using horizontal bars, with the ends of each bar denoting significantly different groups.

orientation of the muscle fibers, and the cross-sectional area of the muscle fibers determine the (passive) muscle stiffness that is generated in certain directions [7]. On the one hand, the erector spinae and abdominal muscles run vertically in the mid-section of the trunk and are responsible for providing forces that facilitate and resist motion in the anterior–posterior direction. The internal and external oblique muscles, on the other hand, run diagonally and wrap around the sides of the trunk, generating forces that codetermine motion in the lateral and diagonal directions. The placement, size, and moment arms of these muscles generate passive forces that may make the movement along the anterior–posterior direction much 'easier' as compared to the lateral displacements. As a consequence of these spine and muscle characteristics, intrinsic trunk stiffness must be a function of displacement direction.

In the context of postural control during sitting, our findings on the direction dependency of trunk stiffness may also shed light on the kinematic behavior of the trunk during sitting. The fact that the center of pressure (COP) fluctuation – an indirect measure for body sway fluctuation [7] – is smaller in the lateral than the anterior–posterior direction [30] can be explained with our current results: the larger the stiffness in a particular direction (i.e., the lateral direction), the smaller the probability for larger trunk displacements. Nevertheless, it should be emphasized that also other mechanisms may contribute to the observed body sway fluctuation during sitting. These include the inhomogeneous shape of the base of support in the anterior–posterior and medial-lateral directions as well as neural control efforts that potentially differ for the two different directions.

4.3. Comparison with previous reports on human trunk stiffness

When comparing the obtained stiffness values with other estimates reported in the literature, significant differences can be found. Translational trunk stiffness for the anterior displacement direction ($k = 1.30 \pm 0.69$ N/mm), for example, was found to be roughly 50% of the value reported by Moorhouse and Granata ($k = 2.20$ N/mm) [15]. However, it has to be emphasized that their objective was to identify trunk stiffness during *active* trunk extensions under a continuous load of 100 N that was superimposed by a pseudorandom force sequence of ±30 N. When the preload was increased from 100 to 135 and 170 N, trunk stiffness increased linearly [15], indicating that *intrinsic* trunk stiffness is proportional to preload. Furthermore, considering the rather impulsive nature of the step perturbation (±30 N), also *reflex* components must have contributed to the stiffness estimates in [15]. Our findings complement these results by showing that trunk stiffness is much lower for small perturbations without preload (typical for natural sitting), suggesting that solely intrinsic stiffness components with low muscle pre-activation levels are at work.

Using a similar experimental paradigm as in [15], Gardner-Morse and Stokes identified translational trunk stiffness during sinusoidal force perturbations that were applied in addition to different steady-state preloads [23]. For a preload of 20% (40%) of the subject's maximum extension force, the stiffness values in the anterior, diagonal, lateral, and posterior directions were approximately 10 times (15 times) larger than the ones in the present study. The fact that the preloads in [23] were even larger than in [15] provides further evidence that trunk stiffness increases with steady-state preload, or effort.

Besides these *translational* stiffness estimations, Cholewicki et al. reported mean *torsional* stiffness values of 500 Nm/rad in the anterior and 600 Nm/rad in the posterior and lateral directions [31]. Again, the identified values were larger than in the present study (about 4 times), likely due to (1) the presence of a high preload of 115 N and (2) the characteristics of the seating apparatus that fixated the lower extremities of the participant [31]. Building upon the results by Kerr and Eng who reported an increase in COP velocity when using a conventional footrest [32], the setup used by Cholewicki et al. may have contributed to the observed muscle activation [31], augmenting both the COP velocity and overall trunk stiffness. As the present study did not use any footrests or fixations, however, the stiffness values reported in Fig. 4A are not affected by such an increase in muscle activation levels.

4.4. Study limitations

The location of the COM was chosen based on a previous study investigating human trunk stiffness [15]. It has to be noted, however, that errors in motion capturing (such as instrumental, artifact-related, and landmark misplacement-related errors) can lead to errors in COM estimations. Further, as we used T10 for COM estimation, we do not account for each individual's trunk shape. A more accurate method for COM estimation is to take high resolution images of each subject's upper body, segment the reconstructed body shell model, and calculate the trunk COM utilizing a continuous trunk density function [33]. In addition, more work is required to quantify errors associated with trunk motion capturing using stereophotogrammetry.

Similar to the COM location, the calculation of the moment of inertia did not consider the geometrical properties of the body. A recent study has shown, however, that the moment of inertia in the lateral direction is higher than in the anterior–posterior direction [33]. Such distinctions could also have an influence on the reported differences between trunk stiffness in the lateral and anterior–posterior directions. Again, a more accurate estimation of the moment of inertia could be obtained for each subject by dissolving the reconstructed body shell model (see above) into small cubic sub-volumes and calculating the 3×3 moment of inertia tensor utilizing the aforementioned trunk density function [33].

While a torsional model was used to consider the vertical displacement of the trunk, the trunk angle required in *Model II* was estimated by capturing only two landmarks, i.e., markers, on each subject's spine. This approach is only valid under the assumption that the L4/L5 joint experiences solely rotational, but no translational motion.

The large standard deviation of the stiffness and damping values could be partially caused by variations in sitting posture. In spite of clear experimental instructions and a spotter ensuring an upright and natural sitting posture, small deviations such as a slight slouch or a lean toward a particular direction may have still occurred, potentially resulting in changes in pulling force. At the same time, it should be emphasized that the variation in stiffness and damping can be, to a larger part, explained by differences in upper body anthropometrics and strength [27].

5. Conclusions

In conclusion, we have developed a novel protocol for quantifying multidirectional trunk stiffness and damping during sitting. This protocol, which allows for subject perturbations in eight different horizontal directions without modifying the experimental arrangement, eliminates the anticipation effect by the subject with respect to timing and direction of the perturbations. Our findings in healthy and young individuals indicate that the stiffness and damping of the trunk, which behaves like a second-order underdamped system, depend on the perturbation direction and are roughly symmetrical between the two body sides. More specifically, both quantities tend to be (1) smallest in the anterior direction and (2) largest in the lateral directions.

Subsequent studies will use the identified stiffness values as a reference for quantifying trunk stiffness in individuals with neurological disorders such as stroke and SCI, but also for assessing whether functional electrical stimulation can be applied to increase trunk stiffness and, hence, trunk stability. In this context, the reported absolute and relative stiffness magnitudes (across different perturbation directions) will be essential for mimicking trunk stiffness in healthy individuals during sitting.

Funding sources

This work was supported by the Canadian Institutes of Health Research (#86427, #94018, and #97953), the CIHR-STIHR Fellowship in Health Care, Technology and Place (HCTP) (TGF-53911), a MITACS Elevate Postdoctoral Fellowship, the University of Toronto, the Toronto Rehabilitation Institute, and the Ontario Ministry of Health and Long-Term Care.

Ethical approval

The study was approved by the Research Ethics Board of Toronto Rehabilitation Institute, Toronto, ON, Canada (reference number: REB05-017). We thank to Mr. Eric Ma for his assistance in the experiments.

Appendix A. Supplementary data

Supplementary data associated with this article can be found, in the online version, at http://dx.doi.org/10.1016/j.medengphy.2013.10.005.

Conflict of interest

There are no conflicts of interest for the authors of this study.

References

[1] Potten YJM, Seelen HAM, Drukker J, Reulens JPH, Drost MR. Postural muscle responses in the spinal cord injured persons during forward reaching. Ergonomics 1999;42:1200–15.
[2] Hsieh C-L, Sheu C-F, Hsueh I-P, Wang C-H. Trunk control as an early predictor of comprehensive activities of daily living function in stroke patients. Stroke 2002;33:2626–30.
[3] Alm M, Gutierrez E, Hultling C, Saraste H. Clinical evaluation of seating in persons with complete thoracic spinal cord injury. Spinal Cord 2003;41:563–71.
[4] Gutierrez EM, Alm M, Hultling C, Saraste H. Measuring seating pressure, area, and asymmetry in persons with spinal cord injury. European Spine Journal 2004;13:374–9.
[5] Chen R, Kayser B, Yan S, Macklem PT. Twitch transdiaphragmatic pressure depends critically on thoracoabdominal configuration. Journal of Applied Physiology 2000;88:54–60.
[6] Anderson KD. Targeting recovery: priorities of the spinal-cord injured population. Journal of Neurotrauma 2004;21:1371–83.
[7] Winter DA. Biomechanics and motor control of human movement. New Jersey City, New Jersey: John Wiley & Sons; 2005.
[8] Kang HG, Dingwell JB. A direct comparison of local dynamic stability during unperturbed standing and walking. Experimental Brain Research 2006;172:35–48.
[9] McGill SM, Grenier S, Kavcic N, Cholewicki J. Coordination of muscle activity to assure stability of the lumbar spine. Journal of Electromyography and Kinesiology 2003;13:353–9.
[10] McGill SM, Cholewicki J. Biomechanical basis for stability: an explanation to enhance clinical utility. Journal of Orthopaedic and Sports Physical Therapy 2001;31:96–100.
[11] Preuss R, Grenier S, McGill SM. Postural control of the lumbar spine in unstable sitting. Archives of Physical Medicine and Rehabilitation 2005;86:2309–15.

[12] Granata K, Orishimo K. Response of trunk muscle coactivation to changes in spinal stability. Journal of Biomechanics 2001;34:1117–23.
[13] Lee PJ, Rogers EL, Granata KP. Active trunk stiffness increases with co-contraction. Journal of Electromyography and Kinesiology 2006;16:51–7.
[14] Stokes IAF, Gardner-Morse M, Henry SM, Badger GJ. Decrease in trunk muscular response to perturbation with preactivation of lumbar spinal musculature. Spine 2000;25:1957–64.
[15] Moorhouse KM, Granata KP. Trunk stiffness and dynamics during active extension exertions. Journal of Biomechanics 2005;38:2000–7.
[16] Cholewicki J, McGill SM. Relationship between muscle force and stiffness in the whole mammalian muscle: a simulation study. Journal of Biomechanical Engineering 1995;117:339–42.
[17] Hogan N. The mechanics of multi-joint posture and movement control. Biological Cybernetics 1985;52:315–31.
[18] Kearney RE, Stein RB, Parameswaran L. Identification of intrinsic and reflex contributions to human ankle stiffness dynamics. IEEE Transactions on Biomedical Engineering 1997;44:493–504.
[19] Nichols T. The contributions of muscles and reflexes to the regulation of joint and limb mechanics. Clinical Orthopaedics and Related Research 2002;403S:S43–50.
[20] Moorhouse KM, Granata KP. Role of reflex dynamics in spinal stability: intrinsic muscle stiffness alone is insufficient for stability. Journal of Biomechanics 2007;40:1058–65.
[21] Masani K, Sin VW, Vette AH, Thrasher TA, Kawashima N, Morris A, et al. Postural reactions of the trunk muscles to multi-directional perturbations in sitting. Clinical Biomechanics 2009;24:176–82.
[22] Lee P, Granata K, Moorhouse K. Active trunk stiffness during voluntary isometric flexion and extension exertions. Human Factors 2007;49:100–9.
[23] Gardner-Morse MG, Stokes IAF. Trunk stiffness increases with steady-state effort. Journal of Biomechanics 2001;34:457–63.
[24] Vette AH, Sanin E, Bulsen A, Morris A, Masani K, Popovic MR. A portable and automated postural perturbation system for balance assessment, training, and neuromuscular system identification. ASME Journal of Medical Devices 2008;2,041007-1 to 41007-9.
[25] Gilles M, Wing AM, Kirker SG. Lateral balance organization in human stance in response to a random or predictable perturbation. Experimental Brain Research 1999;124:137–44.
[26] Cholewicki J, Simons APD, Radebold A. Effects of external trunk loads on lumbar spine stability. Journal of Biomechanics 2000;33:1377–85.
[27] Vette AH, Masani K, Nakazawa K, Popovic MR. Neural-mechanical feedback control scheme generates physiological ankle torque fluctuation during quiet stance. IEEE Transactions on Neural Systems and Rehabilitation Engineering 2010;18:86–95.
[28] Wu N. Quantifying multi-directional trunk stiffness during sitting with and without functional electrical stimulation: Able-bodied subjects. University of Toronto; 2011 [M.A.Sc. Thesis].
[29] Howarth S, Allison A, Grenier S, Cholewicki J, McGill S. On the implications of interpreting the stability index: a spine example. Journal of Biomechanics 2004;37:1147–54.
[30] Vette AH, Masani K, Sin VW, Popovic MR. Posturographic measures in healthy young adults during quiet sitting in comparison with quiet standing. Medical Engineering and Physics 2010;32:32–8.
[31] Cholewicki J, McGill KC, Shah KR, Lee AS. The effects of a three-week use of lumbosacral orthoses on trunk muscle activity and on the muscular response to trunk perturbations. BMC Musculoskeletal Disorders 2010;11:154.
[32] Kerr HM, Eng JJ. Multidirectional measures of seated postural stability. Clinical Biomechanics 2002;17:555–7.
[33] Vette AH, Yoshida T, Thrasher TA, Masani K, Popovic MR. A complete, non-lumped, and verifiable set of upper body segment parameters for three-dimensional dynamic modeling. Medical Engineering and Physics 2011;33:70–9.